Scientific Reports

https://doi.org/10.1038/s41598-026-43807-y

Article in Press

Molecular and spatial heterogeneity of macrophage like vascular smooth muscle cells in abdominal aortic aneurysms associated with intraluminal thrombus

Received: 24 November 2025

Accepted: 6 March 2026

Published online: 16 March 2026

Cite this article as: Ma X., Liang B., Lu Q. *et al.* Molecular and spatial heterogeneity of macrophage like vascular smooth muscle cells in abdominal aortic aneurysms associated with intraluminal thrombus. *Sci Rep* (2026). https://doi.org/10.1038/s41598-026-43807-y

Xiaoying Ma, Bowen Liang, Qingsheng Lu & Chao Song

Molecular and Spatial Heterogeneity of Macrophage Like Vascular Smooth Muscle Cells in Abdominal Aortic Aneurysms Associated with Intraluminal Thrombus

Xiaoying Ma[1,2*], Bowen Liang[1*], Qingsheng Lu[1], Chao Song[1#]

1. Department of Vascular Surgery, Changhai Hospital, Shanghai, China
2. Hepatobiliary Surgery Center, Tongji Hospital, School of Medicine, Tongji University, Shanghai, China

*Contributed equally to this work

#Corresponding author: chao.song@vip.163.com (Chao Song)

To whom correspondence should be addressed:

Chao Song; MD, PhD

Associate Professor, Department of Vascular Surgery, Changhai Hospital, Shanghai, China

168 Changhai Road, Yangpu District, Shanghai 200433, China

Tel: +86 13636392403; Email: chao.song@vip.163.com

Abstract

Abdominal aortic aneurysm (AAA) is a common cardiovascular disease resulting in high mortality rate due to rupture. Intraluminal thrombus (ILT) is involved in AAA progression via both biomechanically protective and biochemically destructive properties. In this study, we utilized multiplex immunofluorescence and GeoMx Digital Spatial Profiler to explore the following issues: (a) Is ILT associated with the phenotypic switching of vascular smooth muscle cells (VSMCs) in aortic aneurysms? (b) Does ILT enrich macrophage-like VSMCs in aortic aneurysms? (c) What role do macrophage-like VSMCs play in aortic aneurysms? We found that the proportion of CD68+SMA+ double-positive cells was significantly increased in AAA with thrombus. Differential gene expression, gene set enrichment and gene signature analyses were performed, in which enrichments were mainly related to VSMC phenotypic switching, matrix remodeling and inflammatory response. The cell-type identification by estimating relative subsets of RNA transcripts (CIBERSORT) was used to quantify the proportions of immune infiltration and the result was that the proportions of naive B cells, M1-type macrophages, and neutrophils were significantly higher in macrophage-like VSMC-rich areas of AAA with ILT. Furthermore, we predicted IL-6 and IL-1β as feature genes which displayed a positive correlation with neutrophil activation. Further, through in vitro assays, we showed that neutrophil extracellular traps (NETs) induce the phenotypic switching of VSMCs through the NF-κB signaling pathway. This study, based on cutting-edge GeoMx Digital Spatial Profiling technology, systematically revealed the cellular and molecular mechanisms underlying the phenotypic switching of VSMCs into macrophage-like cells in AAA associated with ILT. This discovery provides a novel cellular biology perspective for

understanding the destructive role of ILT.

Keywords

Abdominal aortic aneurysm, Intraluminal thrombus, Digital Spatial Profiler, Macrophage-like VSMC, Inflammatory response, Neutrophil activation

1. Introduction

Abdominal aortic aneurysm (AAA) is defined by a pathological and progressive dilation of the infrarenal abdominal aorta, which significantly increases the risk of rupture[3]. The mortality rate for ruptured AAAs can reach as high as 85%[29]. In the past decade, there has been growing recognition of the role of intraluminal thrombus (ILT) in the expansion, remodeling, and rupture of AAA. Early computational models of aneurysm hemodynamics demonstrated that ILT might offer protective benefits by lowering aortic wall stress[15]. However, more recent studies indicate that a higher thrombus burden is associated with an increased rupture risk at smaller AAA diameters[21]. The ongoing debate about whether these damaging biochemical factors outweigh the potential protective effects of reducing mechanical wall stress raises the question of whether antithrombotic therapy aimed at preventing ILT could be beneficial for AAA patients[5, 37].

Recent studies have shown that vascular smooth muscle cells (VSMCs) in aortic aneurysms undergo phenotypic switching. In healthy mature arteries, VSMCs exist in a terminally differentiated and quiescent state known as contractile VSMCs[48], characterized by low proliferation and migration capabilities but high contractile ability[25]. Upon injury or environmental changes, contractile VSMCs lose their contractile markers, such as ACTA2 and MYH11, transitioning to an intermediate state. VSMCs in this intermediate state can differentiate into distinct phenotypes in response to various stimuli[14]. Some phenotypes, such as macrophage-like VSMCs (which express macrophage markers MAC2 and CD68), exhibit features typical of immune cells, including phagocytosis and the secretion of chemokines[4]. This raises questions about the

potential for close communication between immune cells and VSMCs. Evidence suggests that communication between smooth muscle cells (SMCs) and macrophages can lead to an unbalanced secretion of certain matrix proteins by SMCs (including collagen, elastin, and MMP-9), while also promoting the secretion of VEGF and IL-1β, which are known for their angiogenic properties[7]. Recently, our research[38] and that of others[8, 13, 32] have found that interactions between SMCs and monocytes/macrophages trigger an inflammatory cascade that results in monocyte activation and a shift of SMCs toward a synthetic phenotype.

However, three major questions have been raised: (1) Is ILT associated with the phenotypic switching of VSMCs in aortic aneurysms? (2) Does ILT enrich macrophage-like VSMCs in aortic aneurysms? (3) What role do macrophage-like VSMCs play in aortic aneurysms? In this study, we utilized the Multiplex Immunofluorescence (mIF) assay and the GeoMx Digital Spatial Profiler (DSP) platform to explore these questions. The interchangeability of macrophages and VSMCs, along with their crosstalk, suggests that these cell types contribute to the progression of AAA in a more coordinated and interconnected manner than previously thought. This research could potentially reveal new strategies for preventing aortic aneurysm rupture in the context of ILT.

2. Materials and Methods

2.1. Study population

This study was approved by the Ethics Committee of Shanghai Changhai Hospital (approval no. CHEC2022-052) and conducted in accordance with relevant guidelines and regulations. All procedures involving human participants were performed in compliance with the Declaration of Helsinki. Written informed consent was obtained from all patients prior to specimen collection. Open repair of an abdominal aortic aneurysm involved an incision of the abdomen to directly visualize the aortic aneurysm. The procedure was performed in an operating room under general anesthesia. Once the abdomen was opened, the aneurysm was repaired by the use of graft. After the resection of aneurysm (specimen), the graft was sutured to the aorta connecting one end of the aorta at the site of the aneurysm to the other end of the aorta. A cohort of 26 human abdominal aortic aneurysm (AAA) specimens was used for enzyme-linked immunosorbent assay (ELISA) and multiplex immunofluorescence (mIF). An additional 6 AAA tissues were subjected to digital spatial profiling (DSP). The clinical and pathological features of these participants are provided in **Supplementary Tables 1 and 2**.

2.2. Cell culture and reagents

Human aortic vascular smooth muscle cells (HA-VSMCs) were obtained from Pricella Life Science & Technology Co., Ltd. This line, derived from the aortic smooth muscle of an 11-month-old Caucasian female, displays a fibroblast-like phenotype. HA-VSMCs were cultured in Ham’s F-12 K medium supplemented with L-ascorbic acid (0.05 mg/mL), insulin (0.01 mg/mL), transferrin (0.01 mg/mL), sodium selenite (10 ng/mL), endothelial cell growth

supplement (0.03 mg/mL), 10% FBS, 10 mM HEPES, 10 mM TES, penicillin (50 unit/mL) and streptomycin (50 μg/mL). All cellbased assays employed HA-VSMCs at passages 3 to 4. The inhibitors CY-09 (NLRP3 inhibitor, Cat. No. HY-103666) and BAY 11-7082 (NF-κB inhibitor, Cat. No. HY-13453) were sourced from MedChemExpress LLC.

2.3. Isolation of Neutrophils

Neutrophils were isolated from the peripheral blood of healthy volunteers using a neutrophil isolation kit (Cat. No. P9040, Solarbio, China) according to the manufacturer's instructions. The primary neutrophils obtained were maintained in RPMI-1640 medium containing 10% fetal bovine serum. The purity (>98%) and viability (>95%) of the isolated neutrophils were assessed by Giemsa staining and Trypan Blue exclusion assay, respectively.

2.4. In vitro Induction of NETs

Isolated human neutrophils (1×10^7 cells/well) were plated in 6-well plates in serum-free RPMI-1640 medium and allowed to adhere for 1 hour at 37℃, 5% CO_2. NETosis was induced by adding 100 nM phorbol 12-myristate 13-acetate (PMA; Cat. No. P1585, Sigma-Aldrich) and incubating for 4 hours. Following stimulation, the NET-containing supernatant was carefully collected on ice using DNase-free precautions. NETs were then isolated and purified through sequential centrifugation: first at 300 g for 5 min at 4℃ to remove cells and large debris, followed by centrifugation of the resulting supernatant at 10,000 g for 10 min at 4℃. The pellet containing NETs was gently washed once with ice-cold DNase-free PBS, resuspended in a small volume of PBS, aliquoted, flash-frozen, and stored at -80℃ for subsequent experiments.

2.5. ELISA assay of IL-6/IL-1β/MMP-9

Twenty-six AAA tissue samples were harvested and immediately cryopreserved in liquid nitrogen. Aortic tissue lysates were prepared using T-PER tissue protein extraction reagent (Cat, No. 78510, ThermoFisher), and the total protein concentration was determined using Pierce BCA Protein Assay Kits (Cat. No. 23225, ThermoFisher). Additionally, fresh blood was collected from patients using tubes without anticoagulants, allowed to stand at room temperature for 1 hour, then centrifuged at 4°C at 3000 rpm for 10 minutes. Supernatants were maintained at -20°C until analysis. Concentrations of IL-6, IL-1β, and MMP-9 were determined with the following ELISA kits: Human IL6 ELISA Kit (Cat. No. E-EL-H6156, Elabscience), Human IL1β ELISA Kit (Cat. No. E-EL-H0149, Elabscience), and Human MMP9 ELISA Kit (Cat. No. SDH0487, Simuwubio). ELISA assays were conducted following the manufacturer's instructions.

2.6. Multiplex immunofluorescence (mIF) assay

Multiplex immunofluorescence enables the simultaneous detection of multiple protein markers on a single tissue section through sequential rounds of staining and imaging. This technique allows for the spatial profiling of diverse cell types and their phenotypic states within the tissue microenvironment. A total of 26 AAA patients were included. Among them, 14 cases were AAA with mural thrombus, and 12 cases were AAA without mural thrombus. 26 specimens were prepared into formalin-fixed paraffin-embedded tissue (FFPE) samples. The expression of the 5 proteins ACTA2/SMA, CD31, CD68, CD8 and CD20 in cells from formalin-fixed paraffin-embedded tissue samples was examined by multiplex

Immunofluorescence. Tissue sections were incubated with primary antibodies that specifically bind to the target proteins (**details see in Supplementary Table 3**) and with HRP-labelled secondary antibodies that specifically bind to the primary antibodies. This assay was performed by a Bond RX fully automated immunohistochemical stainer and a Vectra Polaris fully automated quantitative pathology imaging system. Scanned images were analysed for positive cell density and proportion using HALO.

2.7. Real-time quantitative reverse transcription-polymerase chain reaction (qRT-PCR)

Total RNA was isolated with the FastPure Cell/Tissue Total RNA Isolation Kit (Vazyme, Cat. No. RC112-01), and reverse transcription was carried out using the AceQ qPCR SYBR Green Master Mix (Vazyme, Cat. No. Q121-02). Quantitative real-time PCR (qPCR) was performed on a CFX96 system (Bio-Rad) with HiScript III SuperMix (Vazyme, Cat. No. R323-01). Primer sequences are listed in **Supplementary Table 4**. Relative mRNA levels were normalized to GAPDH and calculated by the $2^{-\Delta\Delta CT}$ method.

2.8. GeoMx Digital Spatial Profiler (DSP)

The GeoMx DSP platform facilitates spatially resolved, high-plex molecular profiling (transcriptomic or proteomic) from user-defined regions of interest (ROIs) on tissue sections. It bridges histology with molecular data by isolating and collecting nucleic acids or proteins from specific morphological contexts for downstream sequencing or quantification. FFPE sections were hybridized with UV-photocleavable barcode-conjugated RNA in situ hybridization probes to capture and profile mRNA. Specifically, FFPE sections were first stained with SMA and CD68 morphological markers. The

slides were then placed on the GeoMx instrument for ROI selection based on immunofluorescence images. Auto-segmentation was performed using custom UV illumination masks to create AOIs, enabling the release of photocleavable tags specifically from SMA+CD68+, SMA-CD68+, and SMA+CD68- cells. Cleaved barcodes from each AOI were collected and quantified through sequencing. The experiment was supported by JMDNA Bio-Medical Technology Co., Ltd. (Shanghai). The raw sequence data reported in this paper have been deposited in the Genome Sequence Archive[60] in National Genomics Data Center, China National Center for Bioinformation / Beijing Institute of Genomics, Chinese Academy of Sciences (GSA-Human: HRA017020) that are publicly accessible at https://ngdc.cncb.ac.cn/gsa-human.

2.9. Data Quality Control (QC) and data analysis for RNA sequencing

Details see in **Supplementary Methods and Supplemetary Figure 1**.

2.10. Transwell migration assay

HA-VSMCs were treated with 100 ng/mL NETs, and then 2×10^5 cells in serum-free medium were seeded onto 6.5 mm Transwell inserts with 8.0 μm Pore Polycarbonate Membrane (Corning, Cat. No. 3422). For Transwell migration assays, the lower compartment was filled with medium containing 10% fetal bovine serum (FBS) as a chemoattractant. Following 24 h of incubation, cells that had traversed the membrane were fixed with 4% paraformaldehyde, stained with 0.1% crystal violet (Maokangbio, Cat. No. MS4006-100ML), and visualized by microscopy.

2.11. NF-κB Transcription Factor Assay

Nuclear extracts were prepared using the Nuclear Extract Kit (Active Motif, Inc., Cat. No. 40010). DNA-binding activities of cRel, p52, and p65 were quantified with the TransAM NF-κB Transcription Factor Assay Kit (Active Motif, Inc., Cat. No. 43296) according to the manufacturer's instructions. Briefly, 30 µL of Complete Binding Buffer was dispensed per well, followed by 10 µg of nuclear protein diluted to 20 µL. After 1 h incubation at room temperature with orbital shaking (100 rpm), wells were washed thrice with 200 µL 1× Wash Buffer. Primary antibody (1:1000) was added and incubated for 1 h at room temperature, followed by three washes and incubation with HRP-conjugated secondary antibody (1:1000) for another hour. After final washes, 100 µL of Developing Solution was applied and incubated in darkness for 5 min. The reaction was stopped with 100 µL Stop Solution, and absorbance at 450 nm was measured on a BioTek H1MFD microplate reader.

2.12. NFκB Dual Luciferase Reporter Assay

293FT cells in logarithmic growth were plated at 4×10^5 cells/mL in 6-well plates and cultured overnight (37 °C, 5% CO_2). For transfection, 2 µg of NF-κB luciferase reporter plasmid (Yeasen, Cat. No. 11501ES03) was mixed with 125 µL Opti-MEM, and 10 µL Lipofectamine 2000 (Invitrogen, Cat. No. 10668018) was diluted in another 125 µL Opti-MEM. After 5 min incubation at room temperature, the two solutions were combined and left for 20 min to form complexes, which were then added to each well. Following 24 h transfection, cells were reseeded into 96-well plates at 2×10^5 cells/100 µL and incubated overnight. Test compounds were serially diluted 2-fold in culture medium, with a highest concentration of 200 ng/mL and 9 concentration points in total. After 24 hours of

treatment, dual luciferase reporter gene assays were performed following the instructions of the Dual Luciferase Reporter Gene Assay Kit (Yeasen, Cat. No. 11402ES60) and using the Envision 2105 multimode plate reader (PerkinElmer). The results were calculated using the following formula: 1). Experimental Group Ratio = (Experimental Group Firefly Luminescence (F) - Background Firefly Luminescence (F)) / (Experimental Group Renilla Luminescence (R) - Background Renilla Luminescence (R)); 2). Control Group Ratio = (Control Group Firefly Luminescence (F) - Background Firefly Luminescence (F)) / (Control Group Renilla Luminescence (R) - Background Renilla Luminescence (R)); 3). Fold Change = Experimental Group Ratio / Control Group Ratio

Note:

a) Background F: Untransfected cells + Firefly luciferase assay reagent
b) Background R: Transfected cells + Firefly luciferase assay reagent + Renilla luciferase assay reagent
c) Experimental Group: Transfected cells treated with compounds
d) Control Group: Transfected cells without treatment, used for standardization of results

Concentration-response experiments yielded an EC_{50} value of 40.53 μg/mL; accordingly, a working concentration of 100 μg/mL was selected for subsequent cellular assays.

2.13. Statistical analysis

The statistical details of all analyses are reported in the main text, including the statistical test performed and statistical significance. All experimental data were processed with GraphPad Prism 8.0 (GraphPad Software Inc., USA) and expressed as mean ± standard deviation (SD). One-way ANOVA followed by Dunnett's multiple

comparisons test was used to determine differences among multiple groups .The Wilcoxon rank-sum test or unpaired students' t-test (two-tailed) was used to determine differences between two groups. Pearson's correlation coefficient was applied for correlation analysis. A p-value of less than 0.05 was deemed statistically significant.

3. Results

3.1. CD68+/SMA+ cells (macrophage-like VSMC) are enriched in AAA with thrombus

First, we used multiplex immunofluorescence (mIF) technology to compare the proportions of SMA+ and CD68+ cells in AAA with thrombus and AAA without thrombus. SMA+ cells represent vascular smooth muscle cells, while CD68+ cells represent macrophages. As shown in **Figures 1A and 1B**, there was no difference in SMA+ cell density between the two groups; however, in AAA with thrombus, the CD68+ cell density was significantly increased ($P<0.0001$). Macrophage-like VSMCs are named for their similar surface markers and functions to macrophages. These cells contribute to chronic inflammation and may participate in the destruction of the aortic wall. Consistent with our expectations, the proportion of CD68+SMA+ double-positive cells was significantly increased in AAA with thrombus ($P<0.0001$). Additionally, the proportion of CD68+SMA- cells was significantly higher in AAA with thrombus ($P<0.0001$), while the proportion of CD68-SMA+ cells slightly decreased (**Figures 1C-F**). In summary, in AAA with thrombus, the CD68+SMA+ double-positive cells may arise from the conversion of CD68-SMA+ or CD68+SMA- single-positive cells, and this cellular reclassification may be related to inflammation or immune response in AAA with thrombus. Furthermore, we assessed the densities of CD20+ B cells, CD8+ T cells, and CD31+ cells (**Supplementary Figure 2**). In AAA with thrombus, the densities of CD8+ and CD31+ cells were significantly increased ($P<0.0001$), whereas the density of CD20+ cells slightly decreased ($P<0.001$).

3.2. Distinct Transcriptomic Signatures of CD68+SMA+ cells in AAA with or without ILT

To clarify the biological role of CD68+SMA+ cells (macrophage-like VSMCs) in AAA with thrombus at the cellular and molecular levels, we utilized GeoMx Digital Spatial Profiler (DSP) technology for RNA sequencing of specific cell subpopulations. We fixed, embedded, and sectioned tissue samples from three cases of AAA with thrombus and three cases of AAA without thrombus, followed by H&E staining (**Supplementary Figure 3**) and multiplex fluorescence staining (**Figure 2A**), respectively. We selectively outlined the CD68+SMA-, CD68-SMA+, and CD68+SMA+ cell subpopulations using GeoMx Digital Spatial Profiler software (**Figure 2B**).

For CD68+SMA+ double-positive cells, 985 genes were significantly differentially expressed between AAA with thrombus and AAA without thrombus, with thresholds set at FDR (False Discovery Rate) < 0.05 and log2 (Fold Change) > 1. Among these, 778 genes were upregulated and 207 were downregulated (**Figures 3A & 3B**). Notably, IL-6 was significantly upregulated in AAA with thrombus (logFC=5.4). ELISA results indicated that the average IL-6 content in AAA tissue with thrombus was 631±265 pg per mg of total protein, significantly higher than in AAA without thrombus (271±175) (**Figure 3D**). However, most serum samples had IL-6 levels below the detection limit of 0.94 pg/mL (data not shown). Subsequently, we performed GO and KEGG enrichment analyses on the differentially expressed genes using ORA and GSEA methods. The results showed enrichment in phenotypes and signaling pathways, including response to reactive oxygen species, macrophage cytokine production, neutrophil activation, leukocyte aggregation, cytokine-cytokine receptor interaction, TNF signaling pathway, AGE-RAGE signaling pathway, NF-kappaB signaling pathway, MAPK signaling pathway, Ras signaling pathway, HIF-1 signaling pathway, PI3K-Akt

signaling pathway, apoptosis, ferroptosis, and ECM-receptor interaction, and etc (**Figure 3C & Supplementary Table 5**). **Figure 3E** illustrates the differentially expressed cytokines involved in cytokine-cytokine receptor interaction, including IL-6, CCL2, IL-1β and etc. For single-positive cells, details are described in **Supplementary Results 3.2, Supplementary Table 6-7 and Supplementary Figure 4-5.**

3.3. CD68+SMA+ cells display a specific transcriptional regulatory network compared to CD68-SMA+ cells

In AAA with thrombus, we compared the molecular phenotypes of the CD68+SMA+ and CD68-SMA+ cell subpopulations. A total of 77 differentially expressed genes were identified, with thresholds set at FDR < 0.05 and log2 (Fold Change) > 1. Among these, 64 genes were upregulated and 13 genes were downregulated. Notably, MMP-9 (logFC=1.7) and IL-1β (logFC=2.3) were significantly upregulated in AAA with thrombus (**Figures 4A & 4B**). We performed GO and KEGG enrichment analyses on the differentially expressed genes using ORA and GSEA methods. The results indicated enrichment in pathways such as regulation of inflammatory response, neutrophil activation, response to reactive oxygen species, macrophage/monocyte activation, leukocyte aggregation, cytokine-cytokine receptor interaction, TNF signaling pathway, NF-kappaB signaling pathway, AGE-RAGE signaling pathway, and HIF-1 signaling pathway, and etc (**Figure 4C & Supplementary Table 8**). In the cytokine-cytokine receptor interaction analysis, the cytokines with FDR < 0.05 and log2 (Fold Change) > 2 included TNFRSF10C, IL-1β, and CCL8. Additionally, ELISA results indicated that the average IL-1β content in AAA tissue with thrombus was 150±110 pg per mg total protein, significantly higher than in AAA without

thrombus (49±32) (**Figure 4D**). However, most serum samples had IL-1β levels below the detection limit of 4.69 pg/mL (data not shown). Circulating MMP-9 levels showed no significant difference between patient groups (data not shown). In line with this proteolytic phenotype, our previous evaluation of aortic tissue from a related cohort revealed elevated levels of MMP-2, a key protease associated with cell migration, in aneurysms covered with ILT[39]. In AAA without thrombus, we also compared the molecular phenotypes of the CD68+SMA+ and CD68-SMA+ cell subpopulations. Details are described in **Supplementary Results 3.3, Supplementary Table 9 and Supplementary Figure 6.**

3.4. Gene signature analysis of CD68+SMA+ cells in AAA (using Molecular Signatures Database)

Gene signatures represent the expression patterns of single or multiple genes that reflect unique cellular characteristics, often related to physiological or pathological states. In our study, we utilized the Hallmark gene sets from MSigDB to characterize the gene expression data of our gene panel, comprising 50 hallmark gene sets. We employed the Wilcoxon rank-sum test to assess significant differences in signatures between the two groups, with a p-value < 0.05 considered significant. For CD68+SMA+ double-positive cells, several signatures were significantly enriched in AAA with thrombus compared to AAA without thrombus, including Complement, IL6/JAK/STAT3 signaling, inflammatory response, interferon alpha and gamma responses, IL2/STAT5 signaling, PI3K/Akt/mTOR signaling, TGF beta signaling, TNFα signaling via NFκB, apoptosis, and hypoxia (**Figure 5**). In AAA with thrombus, comparisons between CD68+SMA+ and CD68-SMA+ cells revealed significant enrichment of signatures such as Complement,

IL2/STAT5 signaling, TNFα signaling via NFκB, and hypoxia in CD68+SMA+ cells (**Figure 6**). Details are described in **Supplementary Results 3.4 and Supplementary Figure 7-9**.

3.5. Cellular Landscape of Inflammation in CD68+SMA+ cells

The CIBERSORT bioinformatics method was employed to assess the potential abundance of immune cells within specific cell subpopulations. **Figure 7** illustrates the distribution analysis of 22 types of infiltrating immune cells in CD68+SMA+ cells. Compared to AAA without thrombus, the proportions of naive B cells, M1-type macrophages, and neutrophils were significantly higher in AAA with thrombus. In AAA with thrombus, we compared the potential abundance of immune cells in CD68+SMA+ and CD68-SMA+ cells. The proportion of neutrophils in CD68+SMA+ cells was significantly greater than that in CD68-SMA+ cells (**Figure 8A**). We also compared CD68+SMA+ and CD68+SMA- cells in AAA with thrombus. The proportion of naive B cells and neutrophils in CD68+SMA+ cells was significantly greater than in CD68+SMA- cells (**Figure 8B**). Details are described in **Supplementary Results 3.5 and Supplementary Figure 10-13**.

3.6. The association of feature genes with immune cell infiltration in CD68+SMA+ cells

As shown in **Figure 9**, we examined the association between the IL6 / IL-1β genes and infiltrating immune cells using Spearman's rank correlation analysis (**Supplementary Table 10**). IL-6 displayed a positive correlation with activated mast cells (r=0.38, p=0.014), M1 macrophages (r=0.39, p=0.011), and neutrophils (r=0.49, p=0.001), while showing a negative correlation with resting mast cells (r=-0.34, p=0.030). Similarly, IL-1β showed a positive association with

regulatory T cells (Tregs) (r=0.42, p=0.007), neutrophils (r=0.44, p=0.004), and activated mast cells (r=0.71, p<0.0001), along with a negative association with resting mast cells (r=-0.44, p=0.004).

3.7. NETs promote the switching of VSMCs into an inflammatory phenotype through the NF-κB/NLRP3 signaling pathway

Activation of neutrophils leads to the formation of neutrophil extracellular traps (NETs), which capture various enzymes, including proteases, MMP-9, elastase, and pro-oxidative enzymes. Neutrophils were isolated from the peripheral blood of healthy volunteers and induced to form NETs in vitro. After stimulating HA-VSMCs with NETs for 24 hours, qPCR results showed a reduction in the expression of contractile markers MYH11 and Acta2, and an increase in the expression of synthetic markers (KLF4, Opn), matrix metalloproteinases (MMPs), and inflammatory markers (NLRP3, Caspase-1, IL-1B, IL-6) (**Figure 10A**). ELISA results showed that NETs promoted the secretion of IL-1B, IL-6, and IL-18 in HA-VSMCs (**Figure 10B**). Transwell migration assays confirmed that NETs enhanced the migratory ability of HA-VSMCs after 24 hours of treatment (**Figure 10C**). To further validate the induction of a macrophage-like phenotype, we stimulated primary mouse aortic SMCs with NETs. Consistent with the findings in human cells, qRT-PCR analysis revealed a significant increase in the expression of the macrophage marker CD68 in NET-treated mouse SMCs (**Supplementary Figure 14**). The TransAM NF-κB transcription factor assay demonstrated that NETs promoted the protein levels of c-Rel, p52, and p65 in the nucleus of HA-VSMCs (**Figure 10D**). Dual-luciferase reporter assays indicated that NETs activated the NF-κB signaling pathway (**Figure 10E**). Furthermore, the NLRP3 inhibitor

CY-09 and the NF-κB inhibitor BAY11-7082 were able to reverse the activation of the NF-κB pathway induced by NETs in HA-VSMCs (**Figure 10F**).

4. Discussion

The pathogenesis of abdominal aortic aneurysm (AAA) involves a complex interplay between vascular inflammation, extracellular matrix (ECM) remodeling, and phenotypic modulation of vascular smooth muscle cells (VSMCs). Vascular inflammation in AAA involves the chemotaxis of inflammatory cells and the release of pro-inflammatory factors, initiating a cascade of inflammatory responses[59]. Clinically, patients with AAA exhibit elevated levels of circulating pro-inflammatory cytokines[23, 33], and immunohistochemical studies have identified inflammatory cells, including macrophages, T cells, B cells, dendritic cells, natural killer cells, neutrophils, and mast cells, within the aneurysmal wall[2, 44, 54]. The infiltration of inflammatory cells often prompts smooth muscle cells to secrete matrix metalloproteinases (MMPs), which degrade elastin and collagen, reducing arterial wall stability and triggering apoptosis in vascular smooth muscle cells[43].

VSMCs, located in the middle layer of arterial vessels, are essential for maintaining arterial structure and regulating vascular tone. In response to harmful stimuli, some VSMCs lose their contractile protein expression and transition into an intermediate state, which can further differentiate into macrophage-like VSMCs (expressing markers such as MAC2 and CD68)[48]. The interchangeability of macrophages and VSMCs, along with their crosstalk, suggests that these cell types contribute to vascular disease progression in a more integrated manner than previously understood. Our study revealed a marked increase in CD68+SMA+ double-positive cells in AAAs with thrombus, potentially originating from either CD68-SMA+ or CD68+SMA- single-positive precursors. Notably, these dual-positive cells demonstrate specific localization within the adventitia. We

propose that adventitial CD68+SMA+ cells may represent a response to thrombus-associated inflammatory stimuli, possibly involving VSMC migration from media to adventitia, interaction between macrophages & VSMC or cellular transdifferentiation. Besides, co-expression of VSMC-specific markers such as MYH11 (smooth muscle myosin heavy chain) distinguishes these cells from SMA+ activated fibroblasts, underscoring their unique pathobiological significance. It is important to note, however, that VSMCs play complex and dual roles in vascular pathology. Beyond their involvement in inflammatory and destructive processes, VSMCs are also crucial for maintaining vascular structural integrity and can engage in reparative functions. Under certain conditions, VSMCs can increase the synthesis of extracellular matrix (ECM) components, such as collagen, which is essential for providing tensile strength and stabilizing the aortic wall against expansion and rupture[35]. For instance, specific subpopulations of activated mesenchymal cells, including VSMCs and fibroblasts, can upregulate molecules like tumor endothelial marker 1 (TEM1) and enhance collagen production via pathways such as TGF-β/SMAD2 signaling. This profibrotic response represents an intrinsic compensatory mechanism aimed at reinforcing the weakened arterial wall during aneurysm development[24]. Thus, the role of VSMCs, particularly the CD68+SMA+ population observed in our study, may be multifaceted. While they likely contribute to inflammation and matrix degradation as discussed, they may also participate in adaptive or reparative processes. The net impact on aneurysm progression likely depends on the balance between these destructive and protective functions within the local microenvironment.

As early as 1997, Andreeva et al. identified cells co-expressing CD68

and α-SMA in human aortic atherosclerotic plaques, particularly in lipid-rich areas[1]. In contrast to atherosclerosis, where oxidized lipids drive VSMC transformation into foam cells, the ILT in AAA establishes a hypoxic, cytokine-rich niche. Within this environment, we observed a pronounced accumulation of CD68+SMA+ cells, particularly in the adventitia, accompanied by significant neutrophil infiltration. This spatial association suggests that ILT-derived stimuli, such as neutrophil extracellular traps (NETs)—which our in vitro data confirm can induce CD68 expression in VSMCs—play a pivotal role. This mechanism distinguishes AAA from other vascular diseases where VSMC phenotypic shifts are primarily driven by endothelial dysfunction or lipid accumulation, underscoring the unique role of the thrombus as a source of pro-inflammatory mediators. Based on reports in the literature[1, 10-12, 30, 48], we hypothesize that thrombus adjacent to the vessel wall promotes the generation of macrophage-like VSMCs and disrupts the stability of the vascular wall by modulating phenotypes such as inflammation, matrix remodeling, and cell proliferation. Through these mechanisms, ILT not only alters the structure of the vessel but also, through immune responses and matrix degradation, significantly increases the likelihood of aneurysm rupture. Future research should focus on the role and mechanisms of ILT in promoting the generation and phenotypic conversion of macrophage-like VSMCs. Clinically, interventions targeting the generation and phenotypic conversion of macrophage-like VSMCs or inhibiting their interaction with immune cells may offer new strategies for the treatment of AAA.

Neutrophils are abundant in the most luminal layer (blood interface layer) of the intraluminal thrombus (ILT) and the adventitia of AAA[19]. In an experimental animal model, depletion of neutrophils

inhibited AAA formation[17]. Due to their role in the immune-inflammatory response, neutrophils primarily participate in the early inflammatory response and multiple processes of AAA progression, such as oxidative stress, extracellular matrix (ECM) degradation, and ILT formation[40]. As we further explored the role of neutrophils in AAA with concomitant wall thrombus, we noted that in addition to the release of traditional inflammatory cytokines, neutrophils also play an important role in the disease process through the formation of Neutrophil Extracellular Traps (NETs). NETs are net-like structures released by neutrophils, composed of chromatin, histones, and granule proteins[18]. In vivo experiments have shown that inhibiting NET formation (e.g., using DNase, Cl-amidine, GSK484) can effectively slow the progression of AAA[58]. The formation of NETs may serve as a key link in the interaction between neutrophils and VSMCs. After neutrophils release NETs, these NETs not only directly interact with vascular smooth muscle cells but also influence VSMC phenotypic switching (e.g., from contractile to macrophage-like VSMCs). To directly validate the increased neutrophil activity and NETosis inferred from our bioinformatic analyses, we performed multiplex immunofluorescence on human AAA tissue sections. This independent histological assessment confirmed the heightened presence of neutrophils (CD66b+) and NET structures (Citrullinated Histone H3, CitH3+) in ILT-positive AAA. Notably, we observed CD66b+/CitH3+ neutrophils in proximity to, and in some instances infiltrating, CD68+SMA+ double-positive cells. These direct observations corroborate the association between neutrophil/NET infiltration and the macrophage-like VSMC phenotype, providing spatial context to our computational findings. The interaction between neutrophils and VSMCs has not been thoroughly explored. We observed a positive correlation between the expression of classic

inflammatory cytokines IL-6 and IL-1β and neutrophil infiltration in CD68+SMA+ double-positive cells (Figure 9). This result suggests that inflammatory cytokines may play a key role in the interaction between neutrophils and VSMCs. Wall thrombus may promote VSMC phenotypic switching and AAA progression by enhancing neutrophil infiltration and their interaction with VSMCs. Specifically, wall thrombus, through neutrophil infiltration and NET release, may lead to changes in the local inflammatory environment, which in turn promotes VSMC phenotypic transformation, thereby exacerbating aortic wall remodeling and aneurysm expansion.

Both Th1 and Th2 CD4+ T cells, as well as CD8+ T cells, have been implicated in promoting AAA formation[16, 20, 49, 53]. B cells have been found in human AAA for decades and are most frequently located in the adventitia. Potential mechanisms by which B cells may affect AAA include the production of immunoglobulins and cytokines, the regulation of T cells, and the formation of complement components, which may provide the necessary chemotactic signal to recruit neutrophils to the aortic wall[45, 47, 61]. Additionally, B cells produce various cytokines, such as IL-6, TNF-alpha, and IL-10, which are also found in high concentrations in human AAA tissue[41, 55]. These cytokines may mediate the formation and development of human AAA by promoting the activation of lymphocytes or macrophages and mast cells that produce MMPs and cathepsins. In this research, the density of CD8+ cells was significantly increased ($P<0.0001$), while the density of CD20+ cells slightly decreased ($P<0.001$) in AAAs with thrombus. For CD68+ SMA+ cells, the proportion of naive B cells was considerably greater in AAAs with thrombus compared to those without thrombus. In AAAs with thrombus, the proportion of naive B cells in CD68+ SMA+ cells was

considerably greater than in CD68+ SMA- cells. In AAAs without thrombus, we also compared the potential abundance of immune cells in the CD68+ SMA+ and CD68+ SMA- subpopulations. Interestingly, the proportion of naive B cells was considerably lower in CD68+ SMA+ cells compared to CD68+ SMA- cells.

Regarding the molecular pathways responsible for cell cross-talk, previous studies have indicated the activation of signaling pathways such as p38 MAPK and JNK, as well as inflammatory transcription factors like AP-1, NF-κB, and STAT3, in VSMCs and/or monocytes/macrophages following their interactions[9]. In our study, for CD68+ SMA+ double-positive cells, the NF-κB signaling pathway, MAPK signaling pathway, IL-6/JAK/STAT3 signaling, and PI3K/Akt/mTOR signaling were enriched in AAAs with thrombus compared to those without. In AAAs with thrombus, the NF-κB signaling pathway was enriched in CD68+SMA+ double-positive cells relative to CD68- SMA+ single-positive cells. NF-κB, a family of transcription factors, plays a crucial role in both inflammatory responses and oxidative stress, promoting chronic inflammation in the aortic wall and regulating the transcription of MMPs. NF-κB activity is elevated in both human AAA tissues and experimental models of AAA[51], with AngII-induced NF-κB activation identified as a central player in AAA development through the regulation of inflammatory gene expression[22]. Additionally, NF-κB inhibitors have demonstrated significant efficacy in inhibiting AAA formation in animal models[42]. The JAK2/STAT3 signaling pathway is another critical mediator of vascular inflammation during AAA progression. A STAT3 inhibitor (S3I-301) was able to reduce the incidence and severity of AngII-induced AAA formation, decreasing MMP activity and altering the M1/M2 macrophage ratio[46]. These findings

suggest that the JAK2/STAT3 and NF-κB signaling pathways may represent potential therapeutic targets for AAA treatment. Moreover, studies have shown that PI3K inhibitors, such as LY294002 and Gambogic acid, can reduce levels of TNF-α, IL-1β, IL-6, and IL-18, while also suppressing TGF-β, MMP-2, MMP-9, and NF-κB activity. These inhibitors induce VSMC phenotypic conversion and apoptosis, and reduce MMP accumulation in AAA mice, ultimately mitigating the development of aortic aneurysm[34, 36, 52, 56, 57].

This study provides valuable insights into the role of intraluminal thrombus in the progression of abdominal aortic aneurysm, particularly through its effects on vascular smooth muscle cell phenotypic switching. Our findings demonstrate that ILT promotes the accumulation of macrophage-like VSMCs, which contribute significantly to the inflammatory microenvironment in the aneurysmal wall. Differential gene expression analysis and immune cell infiltration profiling revealed that key inflammatory mediators, such as IL-6 and IL-1β, are associated with neutrophil infiltration, suggesting a link between VSMC phenotypic switching and immune response in AAA. These results highlight the critical role of macrophage-like VSMCs in driving inflammation within AAA, offering potential therapeutic targets for modulating these processes.

Beyond these insights, our work directly informs critical avenues for future mechanistic and translational investigation. Mechanistically, the strong association between ILT, neutrophil extracellular traps, and the emergence of CD68+SMA+ macrophage-like VSMCs warrants focused in vivo studies to dissect the precise causal hierarchy and signaling cascades, utilizing tools such as lineage-

tracing models to definitively establish the cellular origin and phenotypic plasticity of these double-positive cells. Furthermore, decomposing the ILT secretome to identify specific factors beyond NETs that drive phenotypic switching could reveal novel druggable pathways. Translationally, the molecular signature of the ILT-associated microenvironment, particularly markers of NETosis (e.g., citrullinated histones, MPO-DNA complexes), should be evaluated in patient plasma as potential prognostic or diagnostic biomarkers to stratify AAA risk or progression. Finally, our data strengthen the rationale for testing therapeutic strategies that target this axis, such as NET inhibition or modulation of the identified NF-κB/STAT3 pathways, moving towards personalized interventions for this high-risk subgroup.

Limitations of this study

While this study was conducted rigorously, we acknowledge its limitations, particularly the need to expand the sample size. The digital spatial profiling analysis, which provided high-resolution spatial transcriptomic data, was performed on a limited cohort of n=3 patients per group with a total of 41 regions of interest (ROIs). Although this approach enabled the discovery of spatially resolved molecular features within specific tissue niches, the sample size constrains the statistical power of these findings and necessitates cautious interpretation. Future validation in larger, independent cohorts is essential to confirm the identified transcriptomic signatures. Besides, future investigations should prioritize mechanistic exploration of molecular drivers underlying VSMC phenotypic switching and their crosstalk with the immune microenvironment, including validation of inflammatory pathways such as TGF-β and NF-κB identified in bioinformatics analyses. A

related and important caveat concerns the cellular origin of the CD68+SMA+ population observed in our multiplex imaging. In the absence of lineage tracing, we cannot definitively distinguish whether these cells represent VSMCs that have acquired CD68 expression or macrophages that have gained SMA expression, as rightly noted in the review process. This fundamental ambiguity underscores the need to elucidate cellular origins through lineage tracing models to resolve debates on macrophage transdifferentiation versus VSMC reprogramming[6, 31]. Furthermore, our conclusion that the intraluminal thrombus is associated with VSMC phenotypic switching is based on correlative evidence from human tissues and supportive but reductionist in vitro models. While new experiments in this revision demonstrate that neutrophil extracellular traps (NETs) can induce CD68 expression in SMCs, these findings do not fully recapitulate the complex in vivo ILT microenvironment nor establish definitive causation in human AAA pathogenesis. Therefore, the relationship should be interpreted as a strong correlation, and future studies employing longitudinal designs or causative interventions in more representative animal models are needed to confirm a direct driving role. Our measurements of systemic inflammatory biomarkers, specifically serum IL-6 and MMP-9, which were low or showed no significant difference between groups in our cohort, contrast with some reports in the literature[50]. This discrepancy likely reflects the considerable clinical heterogeneity among AAA patients (e.g., in aneurysm size, progression rate, comorbidities, and medication use) and underscores that circulating levels may not consistently capture the pathologically relevant, local activity within the aneurysm wall and ILT microenvironment - the primary focus of our investigation. Other key directions include deciphering spatial interactions using

integrated spatial transcriptomics and single-cell RNA sequencing, and characterizing co-localization patterns with fibroblast markers to clarify phenotypic boundaries. Finally, the development of animal models that better mimic human AAA with ILT could help to validate these findings and translate them into clinical applications.

Clinical trial number

Not applicable.

Ethics approval and consent to participate

Clinical samples were collected with ethical approval from the research ethics committee of Shanghai Changhai Hospital (approval no: CHEC2022-052). Informed consent was obtained from all subjects and/or their legal guardian(s).

Acknowledgements

We thank JMDNA Bio-Medical Technology Co., Ltd. (Shanghai) for the support of GeoMx Digital Spatial Profiler study.

Author contributions

XYM and BWL performed the experiments. XYM analyzed data and prepared figures and draft. CS designed/supervised the study and collected clinical samples. XYM and CS applied for the funding. CS and QSL reviewed the manuscript. All the authors approved the submission and publication of the manuscript.

Funding

This work was supported by the Young Scientists Fund of the National Natural Science Foundation of China (Grant No. 82100456 and No. 82400164).

Data availability

The data that support the findings of this study are available from the corresponding author (Chao Song; email: chao.song@vip.163.com) upon reasonable request. The spatial transcriptomic datasets are available in the Genome Sequence Archive (GSA) repository under accession number HRA017020.

Conflict of Interest

The authors declare that the research was conducted in the absence of any commercial or financial relationships that could be construed as a potential conflict of interest.

Reference

1. Andreeva ER, Pugach IM, Orekhov AN (1997) Subendothelial smooth muscle cells of human aorta express macrophage antigen in situ and in vitro. Atherosclerosis 135:19-27
2. Anidjar S, Dobrin PB, Eichorst M, Graham GP, Chejfec G (1992) Correlation of inflammatory infiltrate with the enlargement of experimental aortic aneurysms. Journal of vascular surgery 16:139-147
3. Baman JR, Eskandari MK (2022) What Is an Abdominal Aortic Aneurysm? Jama 328:2280
4. Bennett MR, Sinha S, Owens GK (2016) Vascular Smooth Muscle Cells in Atherosclerosis. Circulation research 118:692-702
5. Boyd AJ (2021) Intraluminal thrombus: Innocent bystander or factor in abdominal aortic aneurysm pathogenesis? JVS-vascular science 2:159-169
6. Boyle JJ, Bowyer DE, Weissberg PL, Bennett MR (2001) Human blood-derived macrophages induce apoptosis in human plaque-derived vascular smooth muscle cells by Fas-ligand/Fas interactions. Arteriosclerosis, thrombosis, and vascular biology 21:1402-1407
7. Butoi E, Gan AM, Tucureanu MM, Stan D, Macarie RD, Constantinescu C, Calin M, Simionescu M, Manduteanu I (2016) Cross-talk between macrophages and smooth muscle cells impairs collagen and metalloprotease synthesis and promotes angiogenesis. Biochimica et biophysica acta 1863:1568-1578
8. Butoi ED, Gan AM, Manduteanu I, Stan D, Calin M, Pirvulescu M, Koenen RR, Weber C, Simionescu M (2011) Cross talk between smooth muscle cells and monocytes/activated monocytes via CX3CL1/CX3CR1 axis augments

expression of pro-atherogenic molecules. Biochimica et biophysica acta 1813:2026-2035

9. Cai Q, Lanting L, Natarajan R (2004) Interaction of monocytes with vascular smooth muscle cells regulates monocyte survival and differentiation through distinct pathways. Arteriosclerosis, thrombosis, and vascular biology 24:2263-2270
10. Cao G, Lu Z, Gu R, Xuan X, Zhang R, Hu J, Dong H (2022) Deciphering the Intercellular Communication Between Immune Cells and Altered Vascular Smooth Muscle Cell Phenotypes in Aortic Aneurysm From Single-Cell Transcriptome Data. Frontiers in cardiovascular medicine 9:936287
11. Cao G, Xuan X, Hu J, Zhang R, Jin H, Dong H (2022) How vascular smooth muscle cell phenotype switching contributes to vascular disease. Cell communication and signaling : CCS 20:180
12. Cao G, Xuan X, Li Y, Hu J, Zhang R, Jin H, Dong H (2023) Single-cell RNA sequencing reveals the vascular smooth muscle cell phenotypic landscape in aortic aneurysm. Cell communication and signaling : CCS 21:113
13. Chen L, Frister A, Wang S, Ludwig A, Behr H, Pippig S, Li B, Simm A, Hofmann B, Pilowski C, Koch S, Buerke M, Rose-John S, Werdan K, Loppnow H (2009) Interaction of vascular smooth muscle cells and monocytes by soluble factors synergistically enhances IL-6 and MCP-1 production. American journal of physiology Heart and circulatory physiology 296:H987-996
14. Chen PY, Qin L, Li G, Malagon-Lopez J, Wang Z, Bergaya S, Gujja S, Caulk AW, Murtada SI, Zhang X, Zhuang ZW, Rao DA, Wang G, Tobiasova Z, Jiang B, Montgomery RR, Sun L, Sun H, Fisher EA, Gulcher JR, Fernandez-Hernando C, Humphrey JD, Tellides G, Chittenden TW, Simons M (2020) Smooth Muscle Cell Reprogramming in Aortic Aneurysms. Cell stem cell 26:542-557.e511
15. Di Martino E, Mantero S, Inzoli F, Melissano G, Astore D, Chiesa R, Fumero R (1998) Biomechanics of abdominal aortic aneurysm in the presence of endoluminal thrombus: experimental characterisation and structural static computational analysis. European journal of vascular and endovascular surgery : the official journal of the European Society for Vascular Surgery 15:290-299
16. Duftner C, Seiler R, Klein-Weigel P, Gî≟bel H, Goldberger C, Ihling C, Fraedrich G, Schirmer M (2005) High prevalence of circulating CD4+CD28- T-cells in patients with small abdominal aortic aneurysms. Arteriosclerosis, thrombosis, and vascular biology 25:1347-1352
17. Eliason JL, Hannawa KK, Ailawadi G, Sinha I, Ford JW, Deogracias MP, Roelofs KJ, Woodrum DT, Ennis TL, Henke PK, Stanley JC, Thompson RW, Upchurch GR, Jr. (2005) Neutrophil depletion inhibits experimental abdominal aortic aneurysm formation. Circulation 112:232-240
18. Fernández-Ruiz I (2018) Inflammation: NETs are involved in AAA. Nature reviews Cardiology 15:257
19. Fontaine V, Touat Z, Mtairag el M, Vranckx R, Louedec L, Houard X, Andreassian B, Sebbag U, Palombi T, Jacob MP, Meilhac O, Michel JB (2004)

Role of leukocyte elastase in preventing cellular re-colonization of the mural thrombus. The American journal of pathology 164:2077-2087

20. Galle C, Schandené L, Stordeur P, Peignois Y, Ferreira J, Wautrecht JC, Dereume JP, Goldman M (2005) Predominance of type 1 CD4+ T cells in human abdominal aortic aneurysm. Clinical and experimental immunology 142:519-527
21. Haller SJ, Crawford JD, Courchaine KM, Bohannan CJ, Landry GJ, Moneta GL, Azarbal AF, Rugonyi S (2018) Intraluminal thrombus is associated with early rupture of abdominal aortic aneurysm. Journal of vascular surgery 67:1051-1058.e1051
22. Hamblin M, Chang L, Zhang H, Yang K, Zhang J, Chen YE (2010) Vascular smooth muscle cell peroxisome proliferator-activated receptor-γ deletion promotes abdominal aortic aneurysms. Journal of vascular surgery 52:984-993
23. Hellenthal FA, Pulinx B, Welten RJ, Teijink JA, van Dieijen-Visser MP, Wodzig WK, Schurink GW (2012) Circulating biomarkers and abdominal aortic aneurysm size. The Journal of surgical research 176:672-678
24. Hong YK, Cheng TL, Hsu CK, Lee FT, Chang BI, Wang KC, Chang LY, Wu HL, Lai CH (2024) Regulation of matrix reloading by tumor endothelial marker 1 protects against abdominal aortic aneurysm. International journal of biological sciences 20:3691-3709
25. Inamoto S, Kwartler CS, Lafont AL, Liang YY, Fadulu VT, Duraisamy S, Willing M, Estrera A, Safi H, Hannibal MC, Carey J, Wiktorowicz J, Tan FK, Feng XH, Pannu H, Milewicz DM (2010) TGFBR2 mutations alter smooth muscle cell phenotype and predispose to thoracic aortic aneurysms and dissections. Cardiovascular research 88:520-529
26. Kanehisa M, Goto S (2000) KEGG: kyoto encyclopedia of genes and genomes. Nucleic acids research 28:27-30
27. Kanehisa M (2019) Toward understanding the origin and evolution of cellular organisms. Protein science : a publication of the Protein Society 28:1947-1951
28. Kanehisa M, Furumichi M, Sato Y, Matsuura Y, Ishiguro-Watanabe M (2025) KEGG: biological systems database as a model of the real world. Nucleic acids research 53:D672-d677
29. Kent KC (2014) Clinical practice. Abdominal aortic aneurysms. The New England journal of medicine 371:2101-2108
30. Klopf J, Brostjan C, Neumayer C, Eilenberg W (2021) Neutrophils as Regulators and Biomarkers of Cardiovascular Inflammation in the Context of Abdominal Aortic Aneurysms. Biomedicines 9
31. Koga J, Aikawa M (2012) Crosstalk between macrophages and smooth muscle cells in atherosclerotic vascular diseases. Vascular pharmacology 57:24-28
32. Li P, Li YL, Li ZY, Wu YN, Zhang CC, A X, Wang CX, Shi HT, Hui MZ, Xie B, Ahmed M, Du J (2014) Cross talk between vascular smooth muscle cells and

monocytes through interleukin-1▓/interleukin-18 signaling promotes vein graft thickening. Arteriosclerosis, thrombosis, and vascular biology 34:2001-2011

33. Lindeman JH, Abdul-Hussien H, Schaapherder AF, Van Bockel JH, Von der Thİ ┗sen JH, Roelen DL, Kleemann R (2008) Enhanced expression and activation of pro-inflammatory transcription factors distinguish aneurysmal from atherosclerotic aorta: IL-6- and IL-8-dominated inflammatory responses prevail in the human aneurysm. Clinical science (London, England : 1979) 114:687-697
34. Liu Q, Shan P, Li H (2019) Gambogic acid prevents angiotensin IIق╣induced abdominal aortic aneurysm through inflammatory and oxidative stress dependent targeting the PI3K/Akt/mTOR and NF▓╣ق╙B signaling pathways. Molecular medicine reports 19:1396-1402
35. Lu H, Du W, Ren L, Hamblin MH, Becker RC, Chen YE, Fan Y (2021) Vascular Smooth Muscle Cells in Aortic Aneurysm: From Genetics to Mechanisms. Journal of the American Heart Association 10:e023601
36. Ma X, Yao H, Yang Y, Jin L, Wang Y, Wu L, Yang S, Cheng K (2018) miR-195 suppresses abdominal aortic aneurysm through the TNF-▓/NF-▓╙B and VEGF/PI3K/Akt pathway. International journal of molecular medicine 41:2350-2358
37. Ma X, Xia S, Liu G, Song C (2022) The Detrimental Role of Intraluminal Thrombus Outweighs Protective Advantage in Abdominal Aortic Aneurysm Pathogenesis: The Implications for the Anti-Platelet Therapy. Biomolecules 12
38. Ma X, Xu J, Lu Q, Feng X, Liu J, Cui C, Song C (2022) Hsa_circ_0087352 promotes the inflammatory response of macrophages in abdominal aortic aneurysm by adsorbing hsa-miR-149-5p. International immunopharmacology 107:108691
39. Ma X, Xu J, Sun H, Liu J, Xia S, Zhang H, Cui C, Song C (2025) Mechanisms of AGE-induced VSMC phenotypic switching and macrophage modulation in human abdominal aortic aneurysms. Experimental biology and medicine (Maywood, NJ) 250:10527
40. Michel JB, Martin-Ventura JL, Egido J, Sakalihasan N, Treska V, Lindholt J, Allaire E, Thorsteinsdottir U, Cockerill G, Swedenborg J (2011) Novel aspects of the pathogenesis of aneurysms of the abdominal aorta in humans. Cardiovascular research 90:18-27
41. Middleton RK, Bown MJ, Lloyd GM, Jones JL, London NJ, Sayers RD (2009) Characterisation of Interleukin-8 and monocyte chemoattractant protein-1 expression within the abdominal aortic aneurysm and their association with mural inflammation. European journal of vascular and endovascular surgery : the official journal of the European Society for Vascular Surgery 37:46-55
42. Miyake T, Aoki M, Masaki H, Kawasaki T, Oishi M, Kataoka K, Ogihara T, Kaneda Y, Morishita R (2007) Regression of abdominal aortic aneurysms by

simultaneous inhibition of nuclear factor kappaB and ets in a rabbit model. Circulation research 101:1175-1184

43. Nie H, Qiu J, Wen S, Zhou W (2020) Combining Bioinformatics Techniques to Study the Key Immune-Related Genes in Abdominal Aortic Aneurysm. Frontiers in genetics 11:579215
44. Ocana E, Bohí╠rquez JC, Pí╙rez-Requena J, Brieva JA, Rodrí╤guez C (2003) Characterisation of T and B lymphocytes infiltrating abdominal aortic aneurysms. Atherosclerosis 170:39-48
45. Pagano MB, Zhou HF, Ennis TL, Wu X, Lambris JD, Atkinson JP, Thompson RW, Hourcade DE, Pham CT (2009) Complement-dependent neutrophil recruitment is critical for the development of elastase-induced abdominal aortic aneurysm. Circulation 119:1805-1813
46. Qin Z, Bagley J, Sukhova G, Baur WE, Park HJ, Beasley D, Libby P, Zhang Y, Galper JB (2015) Angiotensin II-induced TLR4 mediated abdominal aortic aneurysm in apolipoprotein E knockout mice is dependent on STAT3. Journal of molecular and cellular cardiology 87:160-170
47. Ray A, Basu S, Williams CB, Salzman NH, Dittel BN (2012) A novel IL-10-independent regulatory role for B cells in suppressing autoimmunity by maintenance of regulatory T cells via GITR ligand. Journal of immunology (Baltimore, Md : 1950) 188:3188-3198
48. Rong JX, Shapiro M, Trogan E, Fisher EA (2003) Transdifferentiation of mouse aortic smooth muscle cells to a macrophage-like state after cholesterol loading. Proceedings of the National Academy of Sciences of the United States of America 100:13531-13536
49. Schí╧nbeck U, Sukhova GK, Gerdes N, Libby P (2002) T(H)2 predominant immune responses prevail in human abdominal aortic aneurysm. The American journal of pathology 161:499-506
50. Stather PW, Sidloff DA, Dattani N, Gokani VJ, Choke E, Sayers RD, Bown MJ (2014) Meta-analysis and meta-regression analysis of biomarkers for abdominal aortic aneurysm. The British journal of surgery 101:1358-1372
51. Tai HC, Tsai PJ, Chen JY, Lai CH, Wang KC, Teng SH, Lin SC, Chang AY, Jiang MJ, Li YH, Wu HL, Maeda N, Tsai YS (2016) Peroxisome Proliferator-Activated Receptor ċ ╠ Level Contributes to Structural Integrity and Component Production of Elastic Fibers in the Aorta. Hypertension (Dallas, Tex : 1979) 67:1298-1308
52. Takahara Y, Tokunou T, Ichiki T (2018) Suppression of Abdominal Aortic Aneurysm Formation in Mice by Teneligliptin, a Dipeptidyl Peptidase-4 Inhibitor. Journal of atherosclerosis and thrombosis 25:698-708
53. Tang PC, Yakimov AO, Teesdale MA, Coady MA, Dardik A, Elefteriades JA, Tellides G (2005) Transmural inflammation by interferon-gamma-producing T cells correlates with outward vascular remodeling and intimal expansion of ascending thoracic aortic aneurysms. FASEB journal : official publication of the Federation of American Societies for Experimental Biology 19:1528-1530

54. Tsuruda T, Kato J, Hatakeyama K, Kojima K, Yano M, Yano Y, Nakamura K, Nakamura-Uchiyama F, Matsushima Y, Imamura T, Onitsuka T, Asada Y, Nawa Y, Eto T, Kitamura K (2008) Adventitial mast cells contribute to pathogenesis in the progression of abdominal aortic aneurysm. Circulation research 102:1368-1377
55. Vucevic D, Maravic-Stojkovic V, Vasilijic S, Borovic-Labudovic M, Majstorovic I, Radak D, Jevtic M, Milosavljevic P, Colic M (2012) Inverse production of IL-6 and IL-10 by abdominal aortic aneurysm explant tissues in culture. Cardiovascular pathology : the official journal of the Society for Cardiovascular Pathology 21:482-489
56. Wang J, Zhou Y, Wu S, Huang K, Thapa S, Tao L, Wang J, Shen Y, Wang J, Xue Y, Ji K (2018) Astragaloside IV Attenuated 3,4-Benzopyrene-Induced Abdominal Aortic Aneurysm by Ameliorating Macrophage-Mediated Inflammation. Frontiers in pharmacology 9:496
57. Wang Z, Guo J, Han X, Xue M, Wang W, Mi L, Sheng Y, Ma C, Wu J, Wu X (2019) Metformin represses the pathophysiology of AAA by suppressing the activation of PI3K/AKT/mTOR/autophagy pathway in ApoE(-/-) mice. Cell & bioscience 9:68
58. Wei M, Wang X, Song Y, Zhu D, Qi D, Jiao S, Xie G, Liu Y, Yu B, Du J, Wang Y, Qu A (2021) Inhibition of Peptidyl Arginine Deiminase 4-Dependent Neutrophil Extracellular Trap Formation Reduces Angiotensin II-Induced Abdominal Aortic Aneurysm Rupture in Mice. Frontiers in cardiovascular medicine 8:676612
59. Xie S, Ma L, Guan H, Guan S, Wen L, Han C (2020) Daphnetin suppresses experimental abdominal aortic aneurysms in mice via inhibition of aortic mural inflammation. Experimental and therapeutic medicine 20:221
60. Zhang S, Chen X, Jin E, Wang A, Chen T, Zhang X, Zhu J, Dong L, Sun Y, Yu C, Zhou Y, Fan Z, Chen H, Zhai S, Sun Y, Chen Q, Xiao J, Song S, Zhang Z, Bao Y, Wang Y, Zhao W (2025) The GSA Family in 2025: A Broadened Sharing Platform for Multi-omics and Multimodal Data. Genomics, proteomics & bioinformatics 23
61. Zhou HF, Yan H, Stover CM, Fernandez TM, Rodriguez de Cordoba S, Song WC, Wu X, Thompson RW, Schwaeble WJ, Atkinson JP, Hourcade DE, Pham CT (2012) Antibody directs properdin-dependent activation of the complement alternative pathway in a mouse model of abdominal aortic aneurysm. Proceedings of the National Academy of Sciences of the United States of America 109:E415-422

Figures and figure legends

Figure 1

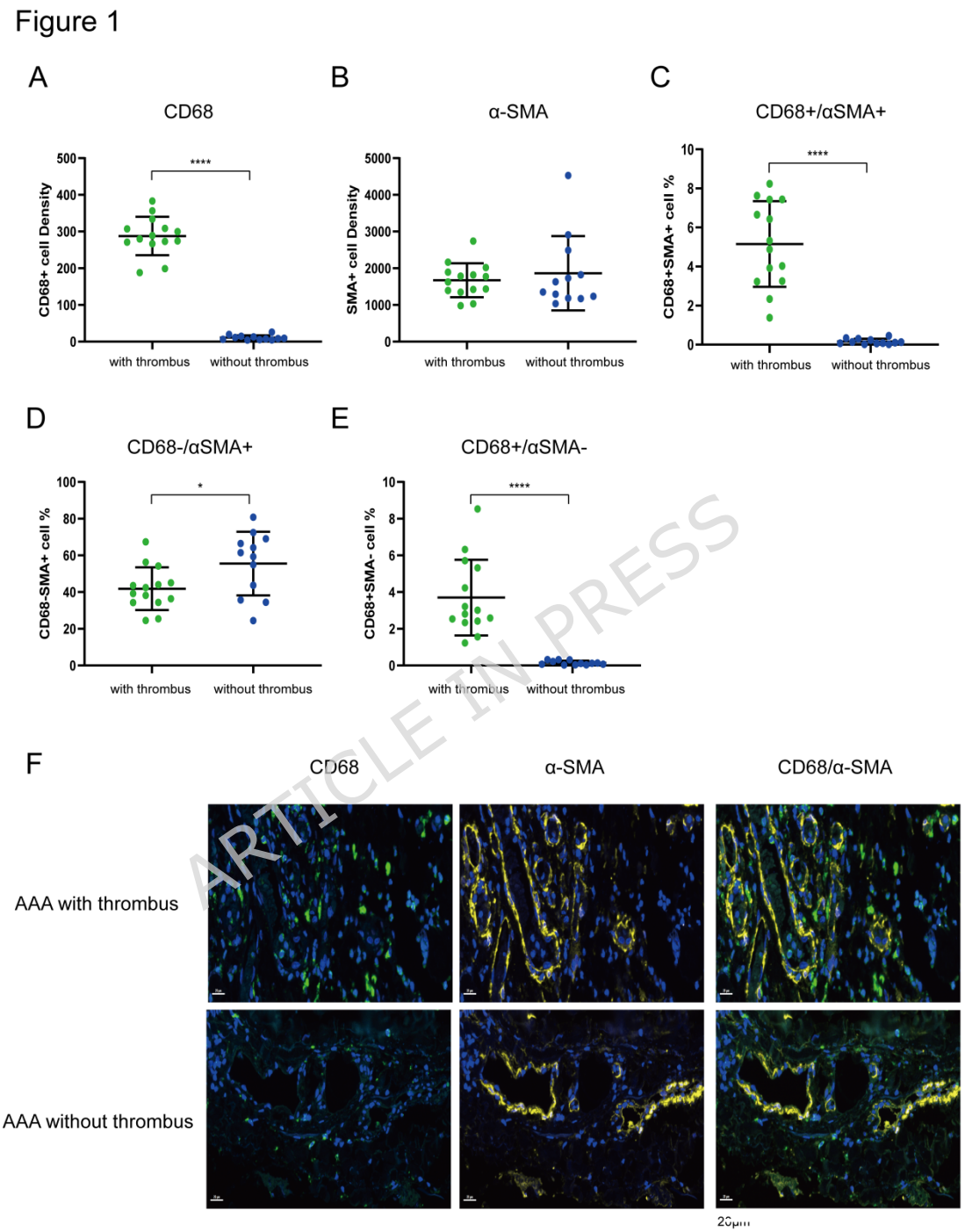

Figure 1. CD68+/SMA+ cells (macrophage-like VSMC) are enriched in AAA with thrombus.

A-E. Multiplex Immunofluorescence (mIF) assay and HALO software analyzed the proportion of double- and single- positive cells in patient AAA with (n=14) or without thrombus (n=12). Data are presented as the mean±standard deviation. The statistical analysis was performed using an unpaired t-test. * indicates P<0.05 and **** indicates P<0.0001. F. Representative images of

mIF. Green fluorescence represents for marker CD68 while yellow for α-SMA. The white solid arrow indicates double-positive cells.

Figure 2

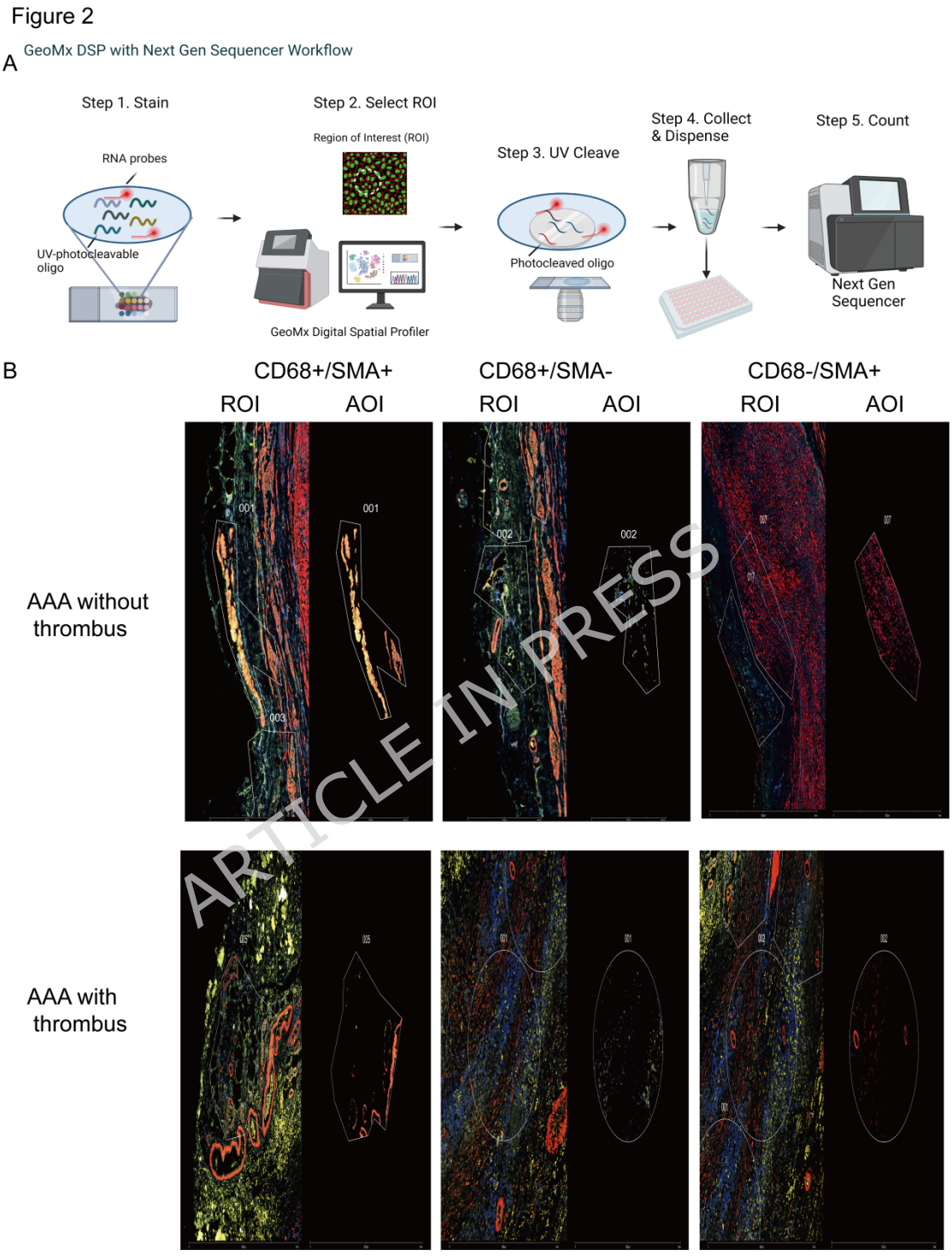

Figure 2. Spatial transcriptomic profiling of AAA tissue using GeoMx Digital Spatial Profiler (DSP)

A. The workflow of GeoMx Digital Spatial Profiler (DSP) with next generation sequencing. B. The ROI (Regions of Interest) and AOI (Areas of Illumination) selection based on immunofluorescence images. This project contains a total of 41 ROIs/AOIs. The numbers in the images represent ROI/AOI labels. The circled ROIs/AOIs represent double-positive or single-positive cell regions.

Green fluorescence represents for marker CD68 while red for α-SMA.

Figure 3

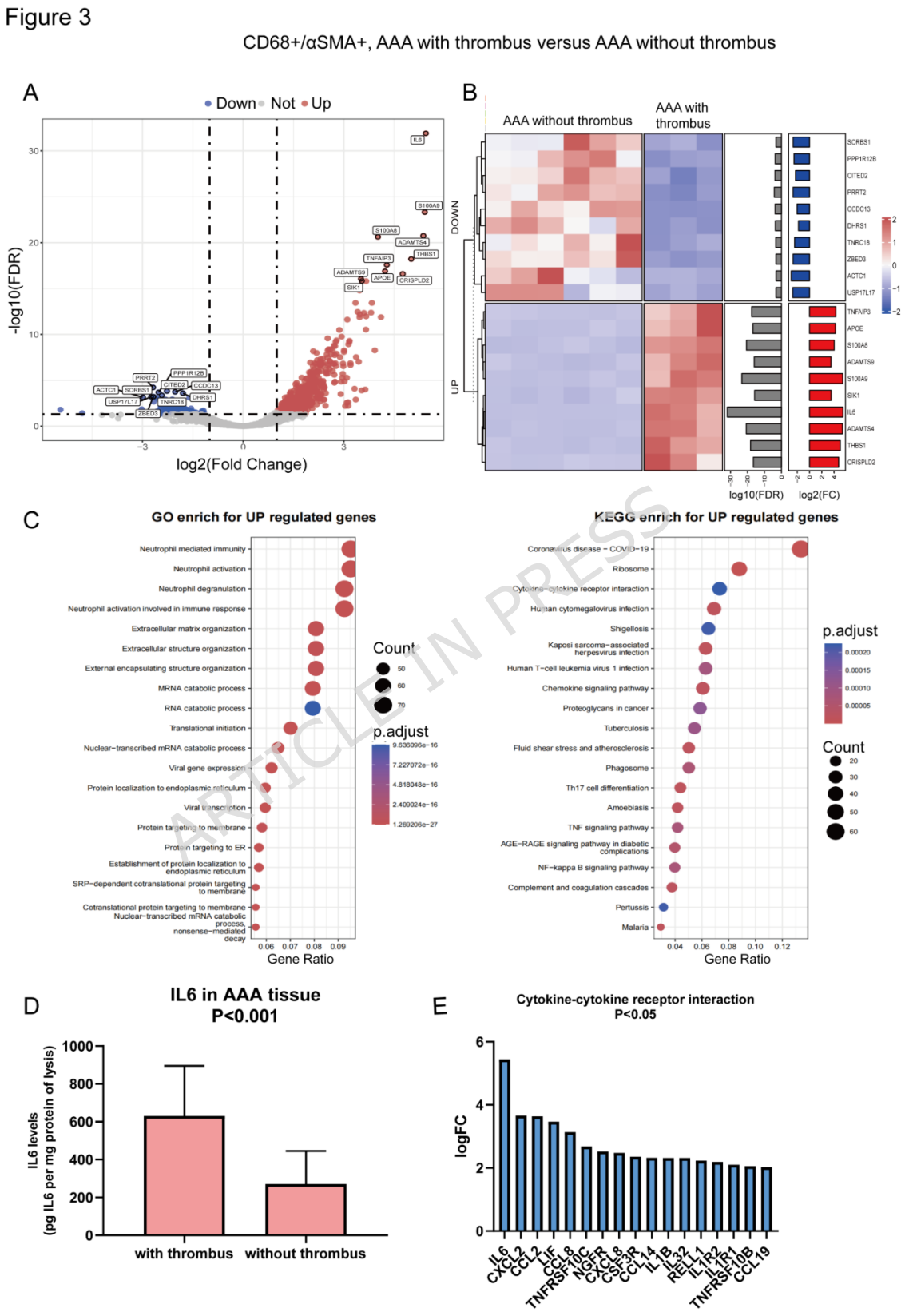

Figure 3. Distinct Transcriptomic Signatures of CD68+SMA+ cells in AAA with or without ILT.

Differential Gene Volcano Plot displayed the Fold Change and FDR (False Discovery Rate) of differentially expressed genes. Genes shown in gray indicate no differential expression in the corresponding analysis, blue points represent downregulated genes, and red points represent upregulated genes. B. A clustering analysis was performed on the obtained differentially expressed genes, and the heatmap displays the results. Red represents up-regulated genes and blue represents down-regulated genes. C. Upregulated genes are subjected to enrichment analysis using Over-Representation Analysis (ORA) for GO/KEGG pathways. The pathway data used in this analysis are derived from the KEGG database (Kanehisa Laboratories)[26-28]. This figure incorporates KEGG pathway imagery/data and is reproduced with permission from Kanehisa Laboratories. D. ELISA results indicated that the average IL-6 content in AAA tissue with thrombus (n=14) was significantly higher than in AAA without thrombus (n=12). Data are presented as the mean±standard deviation. The statistical analysis was performed using an unpaired t-test, ~versus without thrombus, $P<0.001$. E. The differentially expressed cytokines involved in cytokine-cytokine receptor interaction.

Figure 4

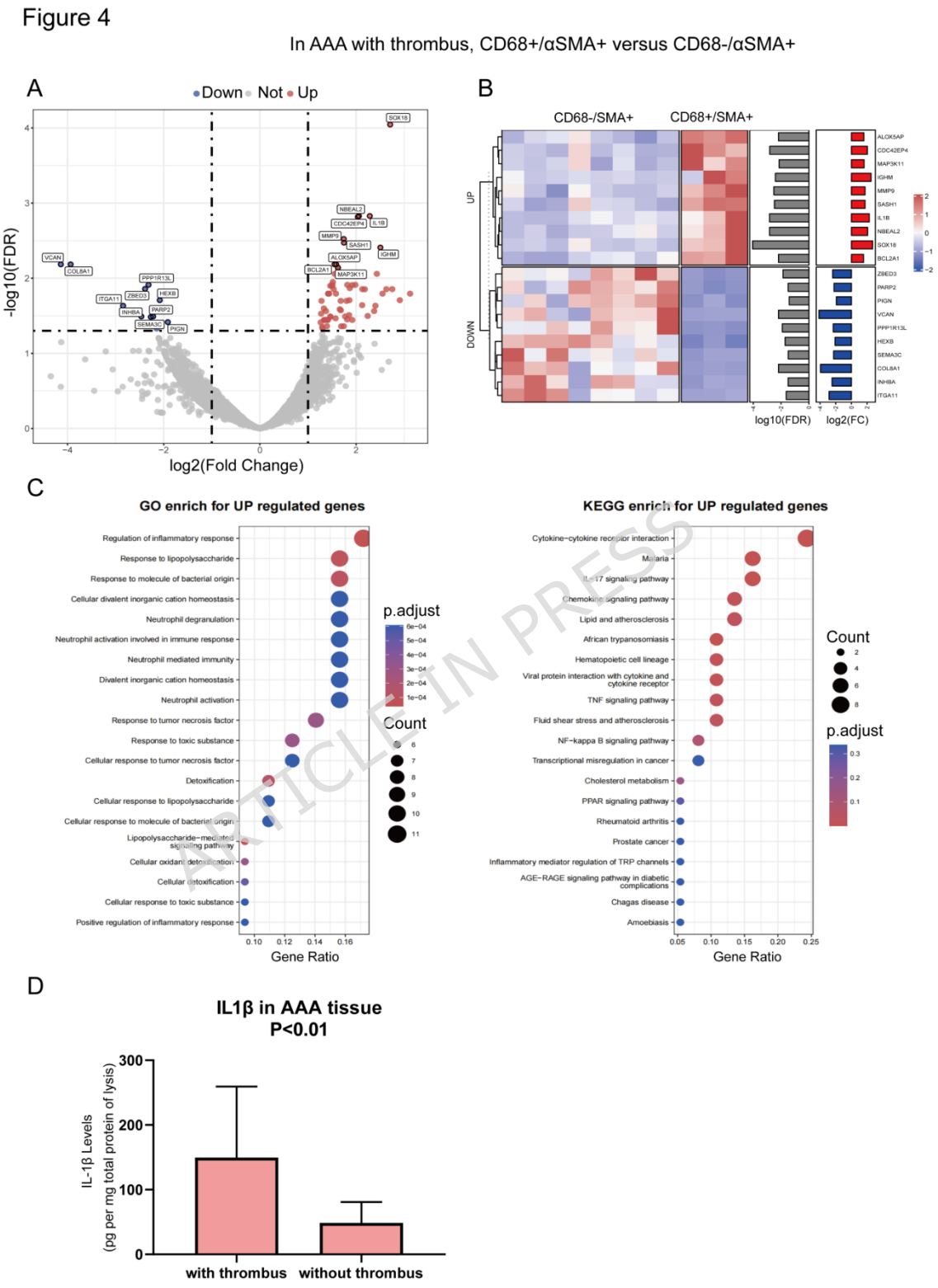

Figure 4. CD68+SMA+ cells display a specific transcriptional regulatory network compared to CD68-SMA+ cells in AAA with thrombus.

A. Differential Gene Volcano Plot displayed the Fold Change and FDR of

differentially expressed genes. Genes shown in gray indicate no differential expression in the corresponding analysis, blue points represent downregulated genes, and red points represent upregulated genes. B. A clustering analysis was performed on the obtained differentially expressed genes, and the heatmap displays the results. Red represents up-regulated genes and blue represents down-regulated genes. C. Upregulated genes are subjected to enrichment analysis using Over-Representation Analysis (ORA) for GO/KEGG pathways. The pathway data used in this analysis are derived from the KEGG database (Kanehisa Laboratories)[26-28]. This figure incorporates KEGG pathway imagery/data and is reproduced with permission from Kanehisa Laboratories. D. ELISA results indicated that the average IL-1β content in AAA tissue with thrombus (n=14) was significantly higher than in AAA without thrombus (n=12). Data are presented as the mean±standard deviation. The statistical analysis was performed using an unpaired t-test, ~versus without thrombus, $P<0.01$.

Figure 5

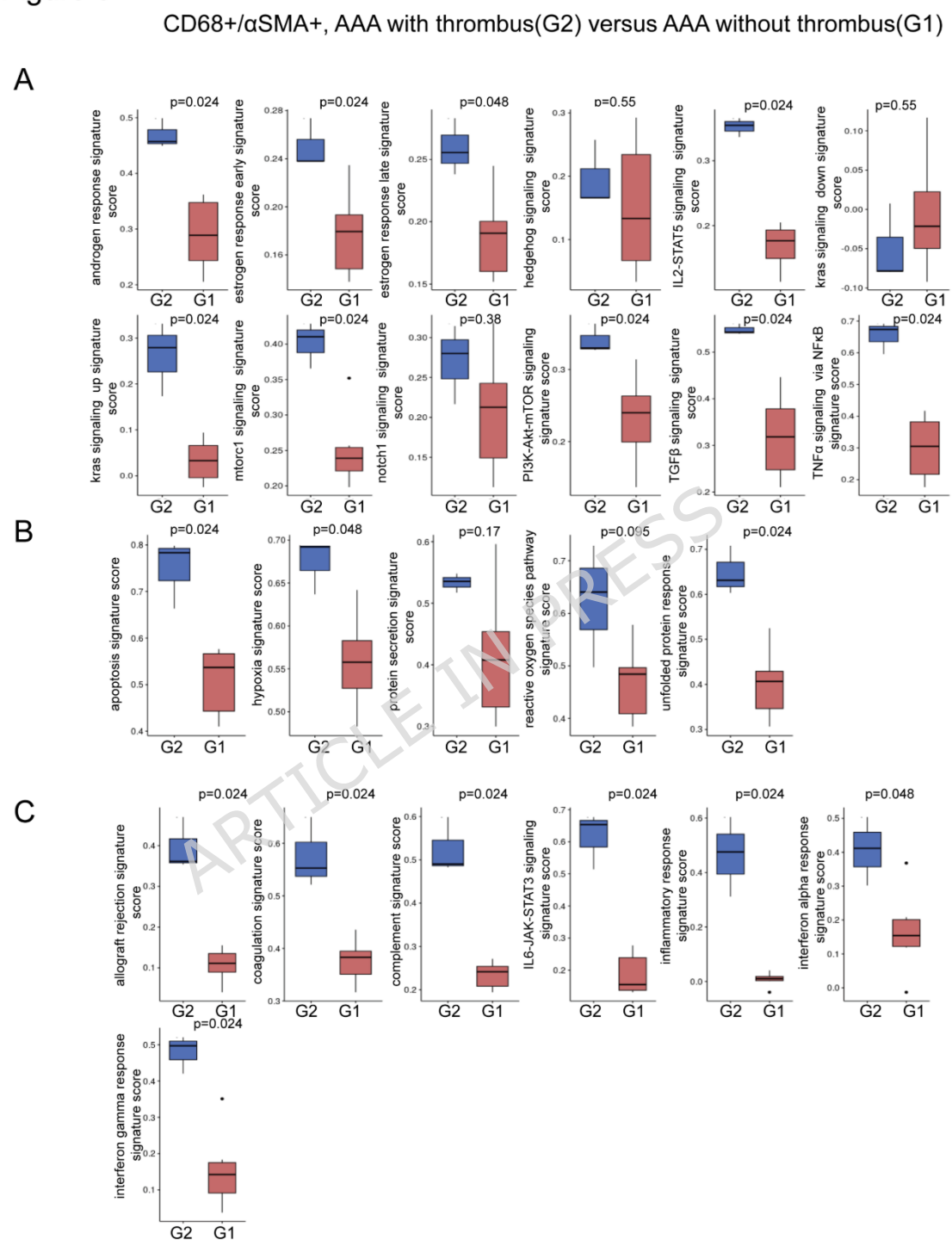

Figure 5. Gene signature analysis of CD68+SMA+ cells in AAA with and without thrombus (using Molecular Signatures Database). The gene expression data utilized known gene sets defined in the MSigDB (Molecular Signatures Database) Hallmark collection, which comprises 50 hallmark gene sets. These gene sets facilitate the identification of specific biological

processes or pathways. This differential analysis focuses on the differential expression of signatures between two groups across (A) Signaling (B) Pathway and (C) Immune. The Wilcoxon rank-sum test is employed to assess whether there are significant differences in each signature between the groups. A p-value < 0.05 is used as the numerical criterion for significance testing.

Figure 6

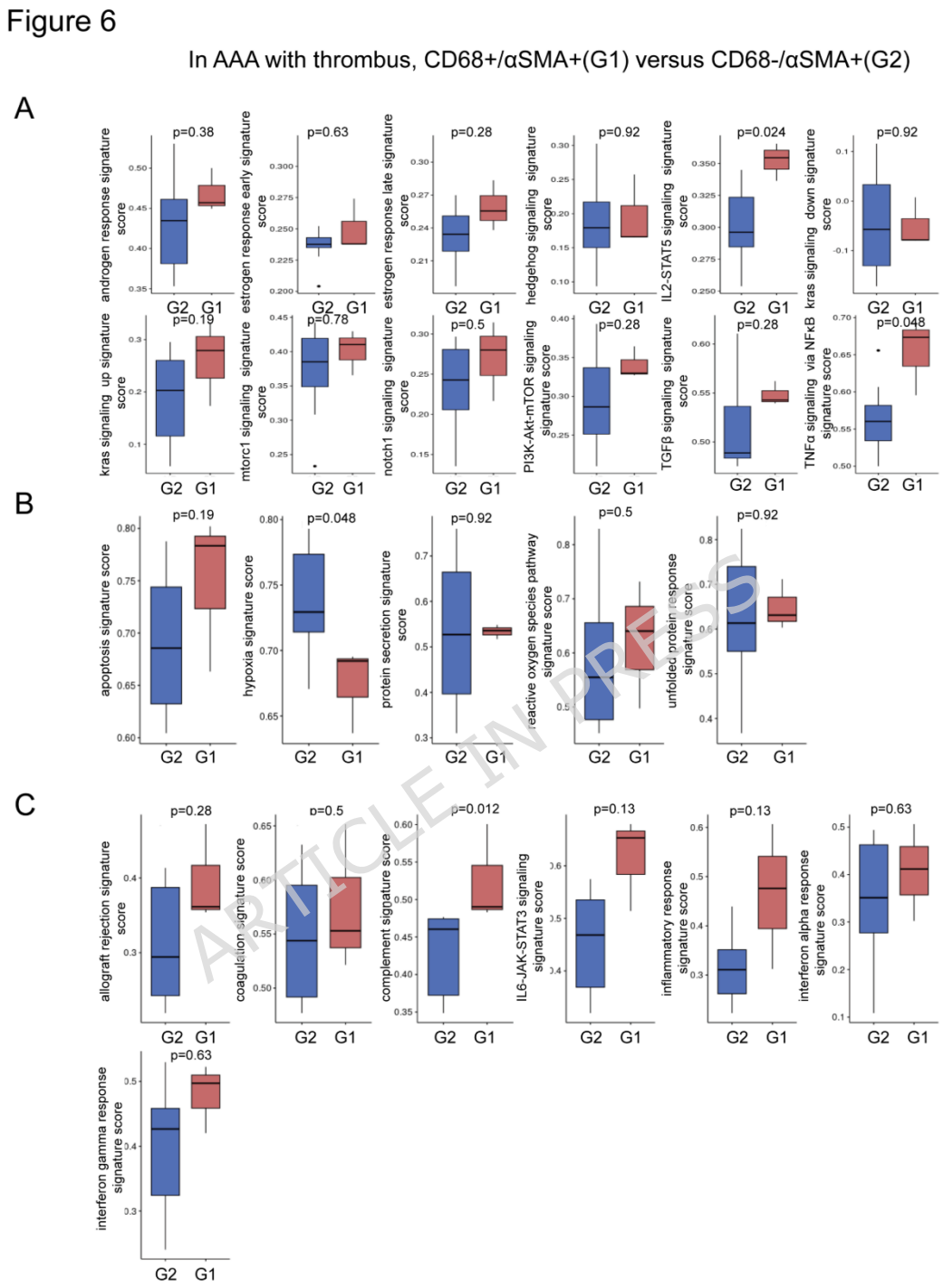

Figure 6. Gene signature analysis of CD68+SMA+ (versus CD68-SMA+) cells in AAA with thrombus (using Molecular Signatures Database).

The gene expression data utilized known gene sets defined in the MSigDB (Molecular Signatures Database) Hallmark collection, which comprises 50 hallmark gene sets. These gene sets facilitate the identification of specific biological processes or pathways. This differential analysis focuses on the differential expression of signatures between two groups across (A) Signaling

(B) Pathway and (C) Immune. The Wilcoxon rank-sum test is employed to assess whether there are significant differences in each signature between the groups. A p-value < 0.05 is used as the numerical criterion for significance testing.

Figure 7

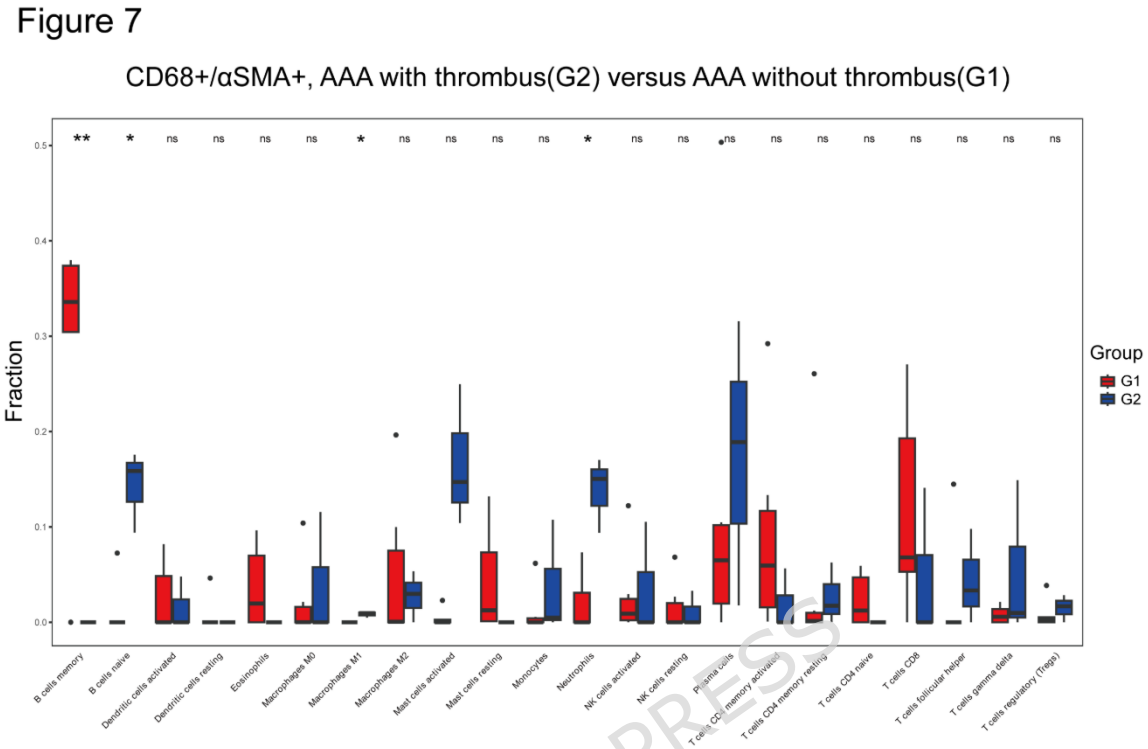

Figure 7. Cellular Landscape of Inflammation in CD68+SMA+ cells (AAA with thrombus versus AAA without thrombus).

Immune cell infiltration was assessed using the bioinformatics tool CIBERSORT (https://cibersortx.stanford.edu/) to compare the relative proportions of various infiltrating immune cell subtypes.

Figure 8

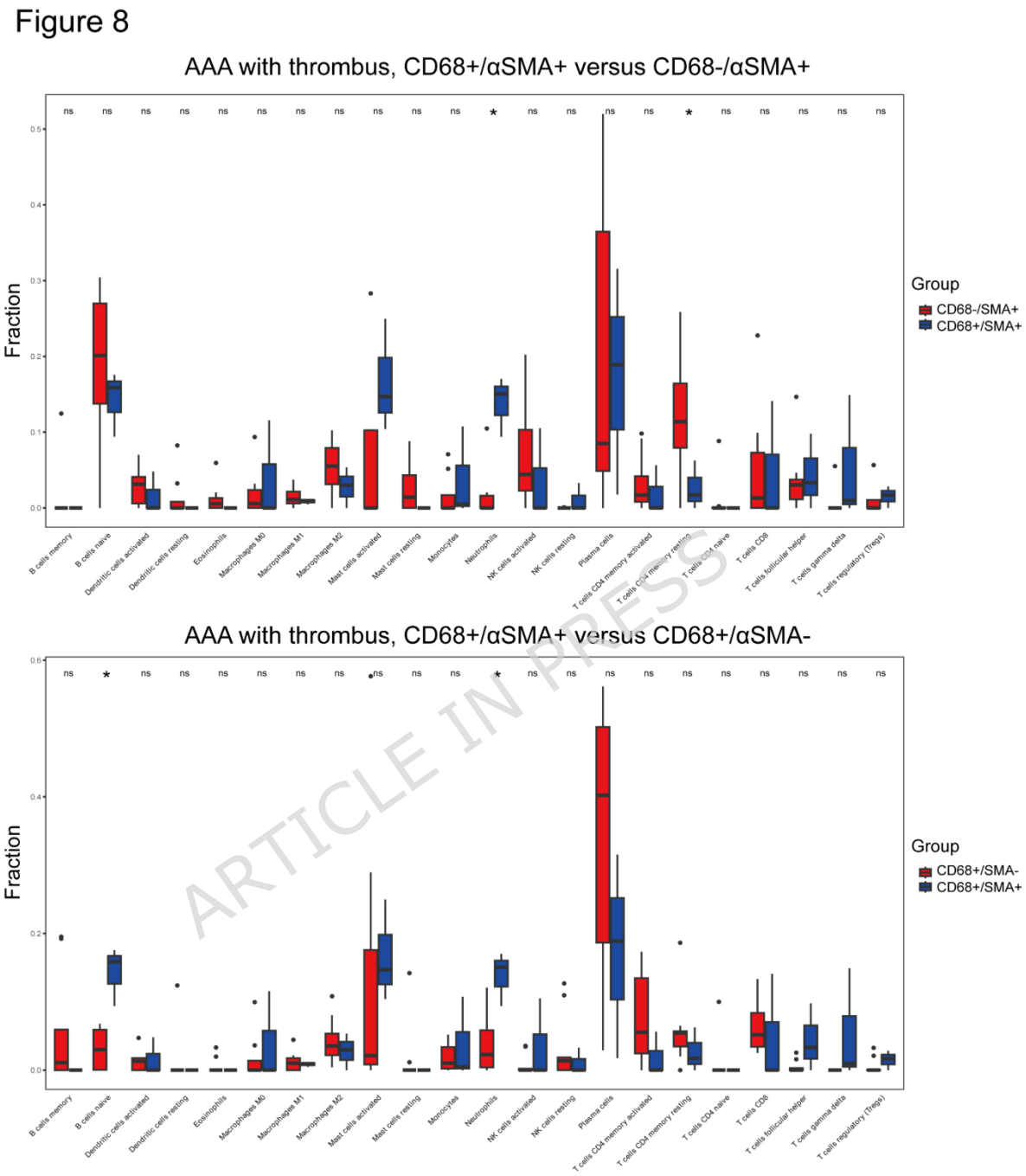

Figure 8. Cellular Landscape of Inflammation in CD68+SMA+ (versus CD68-SMA+ or CD68+SMA-) cells in AAA with thrombus.

Immune cell infiltration was assessed using the bioinformatics tool CIBERSORT (https://cibersortx.stanford.edu/) to compare the relative proportions of various infiltrating immune cell subtypes.

Figure 9

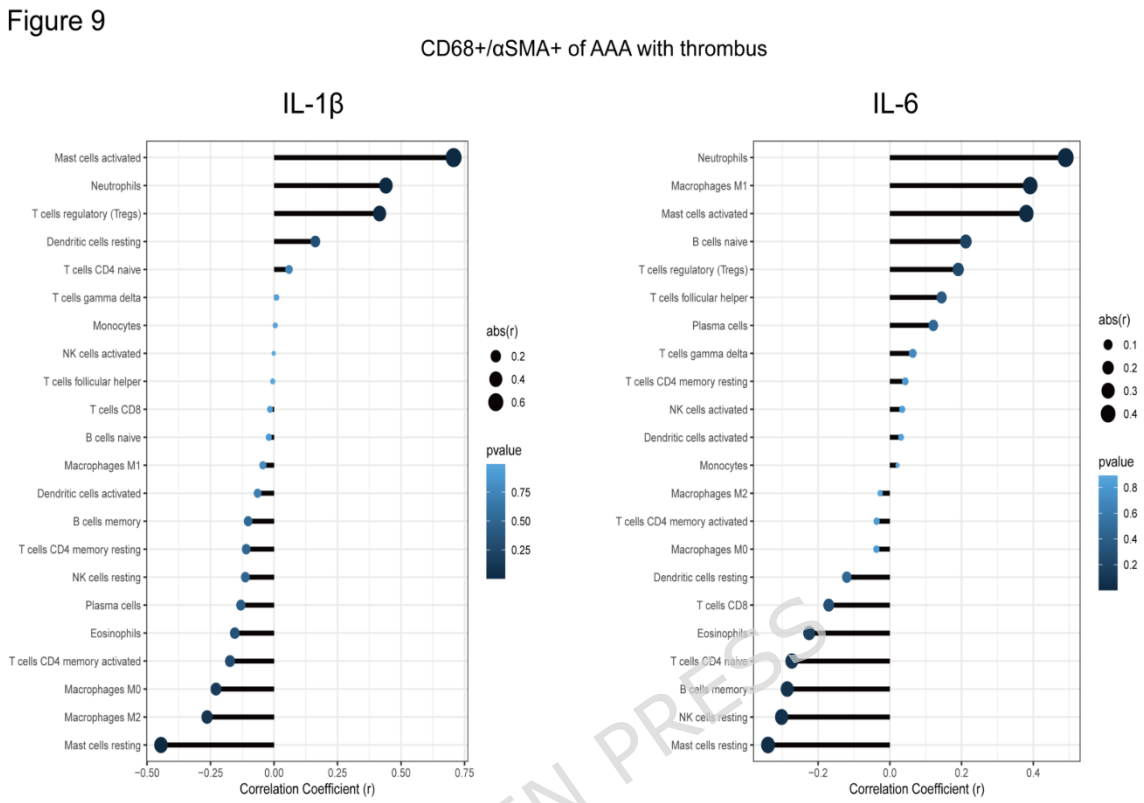

Figure 9. The association of feature genes with immune cell infiltration in CD68+SMA+ cells.

The correlations between the identified features were analyzed using Pearson correlation coefficient tests. IL-6 displayed a positive correlation with activated mast cells (r=0.38, p=0.014), M1 macrophages (r=0.39, p=0.114), and neutrophils (r=0.49, p=0.001), while showing a negative correlation with resting mast cells (r=-0.34, p=0.030). Similarly, IL-1β showed a positive association with regulatory T cells (Tregs) (r=0.42, p=0.007), neutrophils (r=0.44, p=0.004), and activated mast cells (r=0.71, p<0.0001), along with a negative association with resting mast cells (r=-0.44, p=0.004).

Figure 10

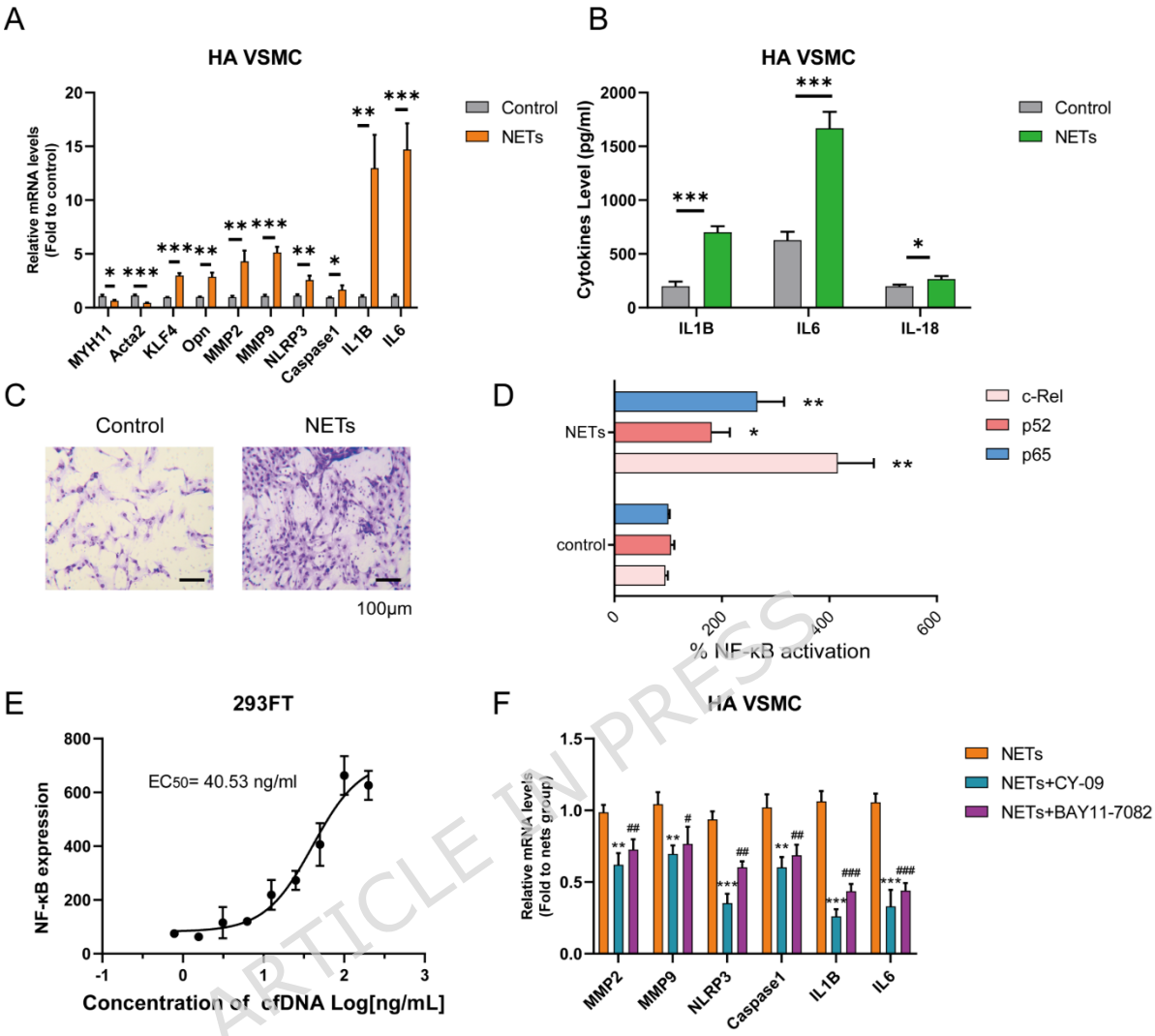

Figure 10. NETs promote the switching of VSMCs into an inflammatory phenotype through the NF-κB/NLRP3 signaling pathway

Neutrophils were isolated from the peripheral blood of healthy volunteers and induced to form NETs in vitro. (A) After stimulating HA-VSMCs with NETs for 24 hours, qPCR results showed a reduction in the expression of contractile markers MYH11 and Acta2, and an increase in the expression of synthetic markers (KLF4, Opn), matrix metalloproteinases (MMPs), and inflammatory markers (NLRP3, Caspase-1, IL-1B, IL-6). (B) ELISA results showed that NETs promoted the secretion of IL-1B, IL-6, and IL-18 in HA-VSMCs. (C) Transwell migration assays confirmed that NETs enhanced the migratory ability of HA-VSMCs after 24 hours of treatment. (D) The TransAM NF-κB transcription factor assay demonstrated that NETs promoted the protein levels of c-Rel, p52, and p65 in the nucleus of HA-VSMCs. (E) Dual-luciferase reporter assays indicated that NETs activated the NF-κB signaling pathway. (F) RT-qPCR was used to validate the effects of the NLRP3 inhibitor CY-09 and the NF-κB inhibitor BAY11-7082 on the expression of MMPs and inflammatory markers

induced by NETs. Data are presented as the mean ± standard deviation (mean ± SD). The results shown in A, B, D, and F are mean ± SD from three independent experiments, each performed with duplicate wells. The statistical analysis was performed using an unpaired t-test. * indicates a significant difference between Nets treatment group and control group or between Nets+CY-09 group and Nets group. # indicates a significant difference between Nets+BAY11-7082 group and Nets group.